

Comparative intra- versus extra-cavity laser cooling efficiencies

Bauke Heeg, Garry Rumbles, Anatoliy Khizhnyak, and Peter A. DeBarber

Citation: [Journal of Applied Physics](#) **91**, 3356 (2002); doi: 10.1063/1.1433922

View online: <http://dx.doi.org/10.1063/1.1433922>

View Table of Contents: <http://scitation.aip.org/content/aip/journal/jap/91/5?ver=pdfcov>

Published by the [AIP Publishing](#)

Articles you may be interested in

[External cavity quantum cascade lasers with ultra rapid acousto-optic tuning](#)

Appl. Phys. Lett. **106**, 141101 (2015); 10.1063/1.4917241

[High power rapidly tunable system for laser cooling](#)

Rev. Sci. Instrum. **83**, 015111 (2012); 10.1063/1.3680612

[Automatic system to control the operation of an extended cavity diode laser](#)

Rev. Sci. Instrum. **75**, 54 (2004); 10.1063/1.1634359

[Continuous pulse duration variation in quenched cavity dye laser](#)

Rev. Sci. Instrum. **74**, 945 (2003); 10.1063/1.1532837

[Laser diode cavity ring-down spectroscopy using acousto-optic modulator stabilization](#)

J. Appl. Phys. **82**, 3199 (1997); 10.1063/1.365688

**SHIMADZU**
Excellence in Science

Powerful, Multi-functional UV-Vis-NIR and FTIR Spectrophotometers

Providing the utmost in sensitivity, accuracy and resolution for applications in materials characterization and nano research

- Photovoltaics
- Polymers
- Thin films
- Paints
- Ceramics
- DNA film structures
- Coatings
- Packaging materials

[Click here to learn more](#)

A row of four Shimadzu spectrophotometers is shown. From left to right: a small benchtop model, a larger benchtop model with a sample holder, a large floor-standing model with a wide sample area, and a tall floor-standing model with a large sample area and a control panel.

Comparative intra- versus extra-cavity laser cooling efficiencies

Bauke Heeg^{a)} and Garry Rumbles^{b)}

Centre for Electronic Materials and Devices, Department of Chemistry, Imperial College, London SW7 2AY, United Kingdom

Anatoliy Khizhnyak and Peter A. DeBarber

Metrolaser Inc., 2572 White Road, Irvine, California 92614

(Received 13 February 2001; accepted for publication 16 November 2001)

Due to recent demonstrations of cooling by anti-Stokes fluorescence the optical geometries under which the cooling efficiency can be optimized are investigated. Since the cooling efficiency is proportional to the absorbed power of radiation, and in previously reported cooling experiments a single pass configuration was mostly used, two schemes for enhancing the absorbed power are compared: placing the cooling medium within the laser resonator and multipassing through an externally located medium. The point of departure in this comparative study is the intracavity circulating intensity, described in terms of the laser gain coefficient and the sum total of losses due to reflections, scatter, and absorption due to the presence of a cooling medium. Substituting measured values of the gain and loss factors for a practical cw pumped dye laser system, a comparison in cooling efficiencies between the two schemes is made for a range of optical densities of the cooling medium. The gain and loss coefficients of a dye laser are measured by introducing a varying loss mechanism by means of an acousto-optic modulator inside the cavity. For high optical densities (>0.1) it was found that when extrapolating the pump power to the dye laser up to 10 W the same cooling power can be achieved with an extra-cavity configuration using relatively few passes as with the intracavity configuration. For low optical densities (<0.01) the number of passes required for equivalent cooling power exceeds 10 and the intracavity configuration becomes a more efficient means for laser cooling. © 2002 American Institute of Physics.
[DOI: 10.1063/1.1433922]

I. INTRODUCTION

Recently, optical cooling of materials by anti-Stokes fluorescence has been demonstrated for an ytterbium-doped fluoride glass, $\text{Yb}^{3+}:\text{ZBLANP}(\text{ZrF}_4\text{-BaF}_2\text{-LaF}_3\text{-AlF}_3\text{-NaF-PBF}_2)$,¹ an acidified Rhodamine 101 solution in ethanol,² and a GaAs quantum well.³ A 65 K drop in temperature from room temperature has been observed with the glass⁴ and cooling has also been found with a similar glass $\text{Yb}^{3+}:\text{ZBLAN}$,^{5,6} where a 48 K drop was observed.⁵ The possibility of making a commercial optical cryocooler working below 77 K has been investigated by several authors^{7,8} as well as compared to some other cooling devices.⁹ In order to reach these temperatures there are several ways to improve the cooling power, which for all systems can be described as

$$P_{\text{applied}} = P_{\text{pump}} A_{\text{dye}} \eta \left[\frac{\lambda_{\text{ave}} - \lambda_{\text{pump}}}{\lambda_{\text{ave}}} \right] + P_{\text{loss}} + P_{\text{load}}$$

$$= P_{\text{cool}} + P_{\text{loss}} + P_{\text{load}}. \quad (1)$$

Symbol P_{pump} is the excitation power, A_{dye} is the fraction of photons absorbed by the dye molecules, η is the quantum yield of fluorescence, λ_{ave} and λ_{pump} are the average fluorescence and excitation wavelengths, respectively

[such that $(\lambda_{\text{ave}} - \lambda_{\text{pump}})/\lambda_{\text{ave}}$ is the average thermal gain per incoming photon, i.e., negative in the case of anti-Stokes fluorescence], P_{loss} is the loss in thermal power due to non-radiative absorption processes, and P_{load} is the sum of contact- and radiative heat loads on the cooling medium. It follows from Eq. (1) that a negative value P_{applied} , corresponding to optical cooling of the sample, can be achieved when $P_{\text{cool}} < -(P_{\text{loss}} + P_{\text{load}})$, since both the thermal load and nonradiative absorption processes result in heating of the sample. In the reported cases of optical cooling P_{pump} has been the maximum available laser output at the time; the output from a dye laser ($\sim 350 \text{ mW}$)² in the case of the dye solutions as cooling medium and the output of a Ti:sapphire (2.2 W)⁴ or laser diode in the case of the glasses. In future devices, compact high power light sources at the wavelength of interest might well be available and therefore provide a means to cool materials down to much lower temperatures. On the other hand, higher pump powers can result in a depletion of the ground state population, N_g , and hence decrease the cooling efficiency. Saturation is enhanced by longer radiative lifetimes, as is the case for most doped glasses (with lifetimes of the order of milliseconds). The fluorescence lifetimes of dyes are, however, very short ($\sim 4 \text{ ns}$ for Rh101), making them amenable to high pump powers such as those inside a laser cavity.

The average gain per photon depends much on the geometry of the cooling medium, since a large volume will enhance fluorescence reabsorption effects that cause a red-

^{a)}Current address: Metrolaser Inc., 2572 White Road, Irvine, CA 92614; electronic mail: bheeg@metrolaserinc.com

^{b)}Corresponding author; electronic mail: g.rumbles@imperial.ac.uk

shift in the fluorescence spectrum and hence decrease the factor $(\lambda_{\text{ave}} - \lambda_{\text{pump}})/\lambda_{\text{ave}}$ to the point where it becomes positive. The effect of radiative energy transfer, or reabsorption effects, on optical cooling has been studied using a stochastic model and will be reported elsewhere.¹⁰ Suffice to mention that the size of a useful cooling sample is limited and as a consequence the heat capacity of the sample is limited. On the one hand a low heat capacity means that one can cool down the sample to lower temperatures,⁴ but on the other hand there will be an enhanced degree of competition with a contact and/or radiative heat load. It is therefore important to be able to use all available light from an excitation source to enhance the overall cooling power and efficiency.

An obvious way to enhance the absorbed radiation is by multipassing the radiation. In the case of the 65 K decrease in temperature, the configuration allowed for two passes of the excitation beam by reflecting off a mirror after passing through the sample.⁴ In the case of the Los Alamos Solid-State Optical Refrigerator (LASSOR) concept,⁵ the excitation source is reflected >200 times within the chamber containing the cooling element by two dielectric mirrors. The requirement of minimizing reabsorption effects means that in a practical multipassing arrangement the retro-reflections should be made as colinear as possible, which is not easy to accomplish for a high number of passes when taking into account the induced thermal lens. It is therefore interesting to compare this multipassing extra-cavity (EC) scheme with the arrangement whereby the cooling sample is placed inside the laser resonator with its inherent colinear multipassing character and hence the relatively easier correction for thermal lens. On the other hand, the cooling sample will induce an additional loss inside the resonator and can therefore substantially lower the intracavity (IC) power and as a result the absorbed power for optical cooling. In this article a comparison is made between the IC and EC configurations, with the gain coefficient of the dye laser as the point of reference between the two systems, and therefore assuming a constant pump power to the dye laser.

In order to be able to compare the two systems, a dye laser with Rhodamine 6G as the gain medium is used, pumped by up to 5 W from an all-lines Ar⁺ laser. It is possible that other light sources such as laser diode arrays will be a viable future alternative in terms of power delivery at the wavelengths of interest (620–630 nm) for cooling of Rhodamine101 solutions. Alternatively, other dyes and consequently different excitation wavelengths might be used. Therefore the present comparison between intracavity and extra-cavity cooling schemes using the Rhodamine 6G dye laser/Rhodamine101 system for evaluation should not be seen as conclusive for other combinations of lasers and cooling media. However, since only gain and loss coefficients are used in this comparison, the same approach is possible for other systems once these coefficients are known.

In the present article we will not include the thermal lens effect, but merely concentrate on the attenuation of radiation in both the IC and EC cooling configuration. This is mainly because the thermal lens will effect both configurations, if not exactly then at least in similar magnitudes.

II. ATTENUATION OF LIGHT IN IC AND EC COOLING SCHEMES

A. Circulating intensity

The circulating intensity for a homogeneously saturated gain medium oscillator in cw operation (for both the IC and EC cooling configuration) is defined by the gain-saturation formula:¹¹

$$I_{\text{circ}} = \left[\frac{g_0}{\delta_e + \delta_{\text{cell}} + \alpha l + \delta_0} - 1 \right] \frac{I_{\text{sat}}}{2}, \quad (2)$$

where g_0 is the unsaturated gain, δ_e is the loss due to the output coupler ($= -\ln[R_{\text{oc}}] \sim T_{\text{oc}}$, where R_{oc} and T_{oc} are the reflectivity and transmission of the output coupler). δ_{cell} is the sum of the loss due to the cell windows of the cooling sample and scatter plus absorption from the solvent and impurities therein. δ_{cell} is therefore the total loss due to cooling sample minus the inherent optical density of the dye solution, αl , α being the absorption coefficient and l the path length of the dye solution. Finally, δ_0 is the total of other intracavity losses, including the losses within the gain medium and other optics, and they are considered to be equal for both IC and EC schemes.

I_{sat} is the saturation intensity of the dye gain medium;

$$I_{\text{sat}} = \frac{\hbar \omega}{\sigma_{21} \tau_{\text{eff}}}, \quad (3)$$

where σ_{21} is the stimulated emission cross section and τ_{eff} the effective fluorescence lifetime of excited molecules within the gain medium, i.e., slightly longer than the lifetime at lower concentrations due to reabsorption effects within the dye-jet. The latter will be denoted as $\tau_f = 1/(k_r + k_{\text{nr}})$, with k_r and k_{nr} being the radiative and nonradiative decay rates. $\tau_r = 1/k_r$ is the radiative or natural lifetime.

For convenience Eq. (2) shall be rewritten as a dimensionless equation;

$$I'_{\text{circ}} = \frac{2I_{\text{circ}}}{I_{\text{sat}}} = \left[\frac{g_0}{\delta_e + \delta_{\text{cell}} + \alpha l + \delta_0} - 1 \right]. \quad (4)$$

In the remainder of the article we will use the prime to denote dimensionless intensities.

B. Absorbed intensity in the intracavity cooling (IC) scheme

For the IC scheme, the normalized intensity absorbed by the dye solution is

$$W_{\text{abs}}^{\text{int}} = I'_{\text{circ}} (e^{\alpha l} - 1). \quad (5)$$

Making the assumption that αl is small and $\delta_e = 0$ (using a high reflector) Eq. (5) can be written as

$$W_{\text{abs}}^{\text{int}} = \alpha l \left[\frac{g_0}{\delta_{\text{cell}} + \alpha l + \delta_0} - 1 \right]. \quad (6)$$

An expression for the optical density for which maximum absorbed power is achieved is found by determining $dW_{\text{abs}}^{\text{int}}/[d(\alpha l)] = 0$. Thus one obtains the expression

$$(\alpha l)_{\text{max}, W} = \sqrt{g_0(\delta_{\text{cell}} + \delta_0)} - (\delta_{\text{cell}} + \delta_0). \quad (7)$$

Substituting Eq. (7) into Eq. (6) leads to the following expression for the maximum absorbed power in the IC scheme;

$$(W_{\text{abs}}^{\text{int}'})_{\text{max}, \alpha l} = (\sqrt{g_0} - \sqrt{(\delta_{\text{cell}} + \delta_0)})^2. \quad (8)$$

C. Absorbed intensity in the extracavity cooling (EC) scheme

The absorbed intensity in the EC scheme is

$$W_{\text{abs}, s}^{\text{ext}'} = \Gamma I_{\text{out}}, \quad (9)$$

where Γ is the fraction of the output power of the laser being absorbed for cooling.

For a single pass through a sample with transmittance T_s the absorbed intensity is

$$\begin{aligned} W_{\text{abs}, s}^{\text{ext}'} &= (1 - T_s) T_w \delta_e I'_{\text{circ}} \\ &= (1 - e^{-\alpha l}) T_w \delta_e \left[\frac{g_0}{\delta_e - \delta_0} - 1 \right], \end{aligned} \quad (10)$$

where T_w is the transmittance of each cell window.

Assuming, as a first approximation, the possibility of multipassing a beam through the sample without distortion of the beam profile, with each pass comprising two passes through the cell window followed by one reflection at a mirror (with a reflectivity R), the intensity after N passes, I_N , is defined as

$$I_N = I_0 (\theta T_s)^N, \quad (11)$$

where $\theta = (T_w)^2 R$.

The absorbed intensity during the n th pass through the cell is (note the inclusion of the attenuation T_w)

$$W_{\text{abs}, n}^{\text{ext}'} = I_{n-1} T_w (1 - T_s) = I_0 T_w (1 - T_s) (\theta T_s)^{n-1}. \quad (12)$$

The total absorbed intensity in the multipass EC scheme after N passes can therefore be written as

$$\begin{aligned} W_{\text{abs}}^{\text{ext}'} &= \sum_{n=1}^N W_{\text{abs}, n}^{\text{ext}'} = I_0 T_w (1 - T_s) \sum_{n=1}^N (\theta T_s)^{n-1} \\ &= I_0 T_w (1 - T_s) \frac{1 - (\theta T_s)^N}{1 - \theta T_s}. \end{aligned} \quad (13)$$

Optimizing the output coupler ($dI'_{\text{circ}}/d\delta_e = 0$) for maximum I_0 gives

$$(\delta_e)_{\text{opt}} = \sqrt{g_0 \delta_0} - \delta_0. \quad (14)$$

Hence the optimized absorbed intensity, maximized for the output coupler, in the EC scheme is defined as

$$(W_{\text{abs}}^{\text{ext}'})_{\text{opt}} = (\sqrt{g_0} - \sqrt{\delta_0})^2 T_w (1 - T_s) \frac{1 - (\theta T_s)^N}{1 - \theta T_s}. \quad (15)$$

There is no equivalent to Eq. (8) for the EC scheme since the absorbed intensity increases continuously with optical density. In summary the IC and EC schemes are not equivalent because when changing the optical density in the IC scheme one has to change the condition of laser oscillation (i.e., for an optimum absorbing condition one has to change the intracavity losses), whereas in the EC case increas-

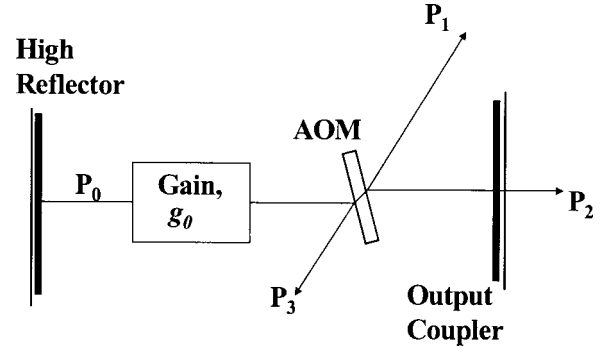


FIG. 1. Arrangement for the measurement of dye laser gain and loss values, using an acousto-optic modulator, after Ref. 12. P_1 and P_3 are the diffracted beams, P_2 is the output beam, and P_0 is the intracavity laser beam.

ing the optical density automatically increases the absorbed power. By using Eqs. (6) and (15) we can compare absorbed power for a range of values for αl , and thus it can be estimated how many passes in the EC scheme (for a given value of αl) equate the IC absorbed intensity. In order to do so, realistic values for the unsaturated gain, intracavity losses, and extra-cavity losses are required.

III. MEASUREMENT OF g_0 AND δ_0 IN A PRACTICAL DYE LASER SYSTEM

The technique used for measuring g_0 and δ_0 is very similar to that reported elsewhere.¹² An acousto-optic modulator (AOM) is placed inside the laser resonator as in Fig. 1. Rather than creating a continuously variable transmission mirror by varying the rf voltage across the AOM as described in Ref. 12, a pseudo-continuously variable transmission mirror is achieved by applying an rf pulse (Coherent Cavity Dumper driver 7200) at frequencies f_{AOM} ranging from 0.15 to 9.5 MHz.

As in Ref. 11, one can define the power extraction efficiency (per pass) as the ratio of diffracted versus input power;

$$\eta_{\text{AOM}}(f_{\text{AOM}}) = \frac{I_{\text{diff}}(f_{\text{AOM}})}{I_{\text{in}}}, \quad (16)$$

and the transmission of the AOM as

$$T_{\text{AOM}} = 1 - \eta_{\text{AOM}}(f_{\text{AOM}}). \quad (17)$$

The equivalent reflectivity R_{eq} is defined as

$$R_{\text{eq}} = R_{\text{oc}} T_{\text{AOM}}^2, \quad (18)$$

where R_{oc} is the reflectivity of the output coupler. The total output power P is then given by

$$P = P_0 (1 - R_{\text{eq}}), \quad (19)$$

where P_0 is the intracavity power.

It should be noted that P_0 is considered to be the same on both sides of the AOM, which is not strictly correct but since T_{AOM} is nearly 1.0 this assumption is justifiable in the present case. P expressed in terms of P_3 is

$$P = \frac{P_3 (1 - R_{\text{eq}})}{R_{\text{oc}} T_{\text{AOM}} - R_{\text{eq}}}. \quad (20)$$

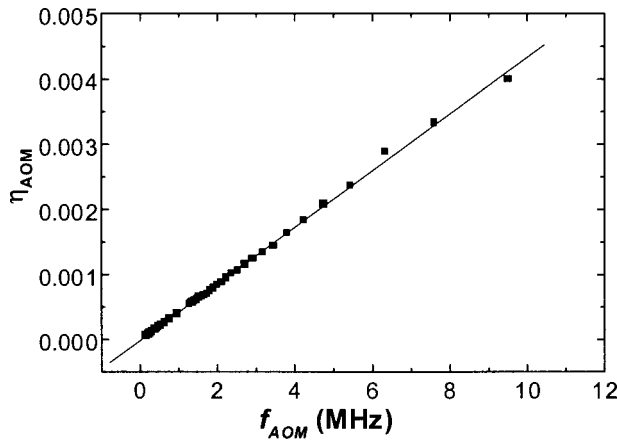


FIG. 2. Power extraction efficiency of the acousto-optic modulator vs rf pulse frequency, as measured using a cavity dumper driver.

Hence by measuring P_3 for different f_{AOM} , substituting a value for R_{oc} and calibrating η_{AOM} one obtains a plot of P versus R_{eq} which, by fitting with

$$P = \left(\frac{AI_{\text{sat}}}{2} \right) (-\ln[R_{\text{eq}}]) \left[\frac{g_0}{\delta_0 - \ln[R_{\text{eq}}]} - 1 \right], \quad (21)$$

gives the parameters g_0 and δ_0 . In order to fit the data correctly, the amplitude coefficient, $\Omega = AI_{\text{sat}}/2$, has to be estimated.

IV. EXPERIMENTAL RESULTS

A. Amplitude coefficient

The amplitude coefficient $AI_{\text{sat}}/2 = Ah\nu/2\tau_{\text{eff}}\sigma_{21}$ is estimated as follows: The effective lifetime is measured using time-resolved single photon counting on the dye solution in a 1 mm path-length cuvette (in order to minimize reabsorption effects) with an excitation wavelength of 330 nm. After deconvolution of the instrument response and fitting to a single-exponential decay function, a measured fluorescence lifetime, τ_{eff} , of 7.84 ns is obtained.

The stimulated emission cross section σ_{21} is estimated from the fluorescence spectrum of the dye solution using

$$\sigma_{21} = \frac{\lambda^4 F_0(\lambda)}{8cn_D^2 \pi \tau_f}, \quad (22)$$

where $F_0(\lambda)$ is the normalized molecular fluorescence of Rh6G (i.e., at low concentrations in order to exclude reabsorption effects), n_D the refractive index of the solution, and τ_f the fluorescence lifetime of the dye, estimated to be 4.6 ns. This results in an estimated value for σ_{21} of $2.5 \times 10^{-16} \text{ cm}^2$ at 620 nm, which is the wavelength at which maximum cooling is predicted. Further, assuming a beam-waist of the focused pump beam of 25 μm , this yields a value of 1.6 W for the amplitude coefficient Ω .

B. Extraction efficiency of AOM, η_{AOM}

Using 450 mW of input power, the extraction power efficiency, η_{AOM} , as a function of f_{AOM} for the AOM is measured, see Fig. 2. The fitted curve has the form $\eta_{\text{AOM}} = -1.19 \times 10^{-5} + 4.35 \times 10^{-10} f_{\text{AOM}}$.

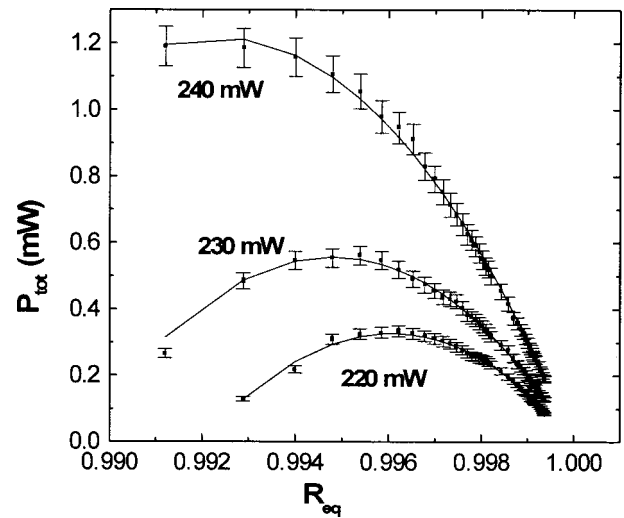


FIG. 3. Total output power as a function of equivalent reflectivity of the combined AOM/output coupler as calculated and fitted with Eqs. (19) and (20), respectively.

C. Variable transmission measurements in resonator

Next, the AOM is placed inside the resonator of a Coherent 599 series dye laser using only broadband high reflector optics, i.e., the output coupler was replaced by a high reflector mirror. f_{AOM} is set at 9.5 MHz and the input power (Ar^+ , all lines), P_{in} , is minimized while bringing the dye laser to threshold lasing. This resulted in a minimum pump power of 220 mW. Then P_3 is measured as a function of f_{AOM} and P is calculated with Eq. (20) and fitted with Eq. (21), using $\Omega = 1.6 \text{ W}$ and assuming a value for the reflectivity of the output coupler $R_{\text{oc}} = 0.9995$. The results are shown in Fig. 3.

The procedure was repeated for higher pump powers in order to test whether g_0 increases linearly with P_{in} as predicted and how δ_0 and $\Delta = (g_0 - \delta_0)$ vary with increasing input power. From the fitted curves values for gain and loss are given in Table I. The data are seen to deviate from linearity at high powers and this is due to a decrease in the laser mode area at high powers.

The variation of g_0 and δ_0 with pump power is shown again graphically in Fig. 4. For convenience, the plots are given in terms of $(1 - g_0)$ and $(1 - \delta_0)$ versus P_{in} , in order that an extrapolation towards high pump powers (10 W) can

TABLE I. Gain, g_0 , and loss, δ_0 , parameters for several input powers to the dye laser, obtained by fitting experimental data obtained through Eq. (20) with Eq. (21).

P_{in} (W)	g_0	δ_0	$\Delta = g_0 - \delta_0$
0.22	0.084	0.076	0.008
0.23	0.089	0.078	0.011
0.24	0.095	0.079	0.016
0.28	0.089	0.066	0.022
0.33	0.104	0.066	0.038
0.41	0.094	0.049	0.044
0.60	0.117	0.040	0.077
1.4	0.168	0.029	0.139
2.4	0.207	0.025	0.182

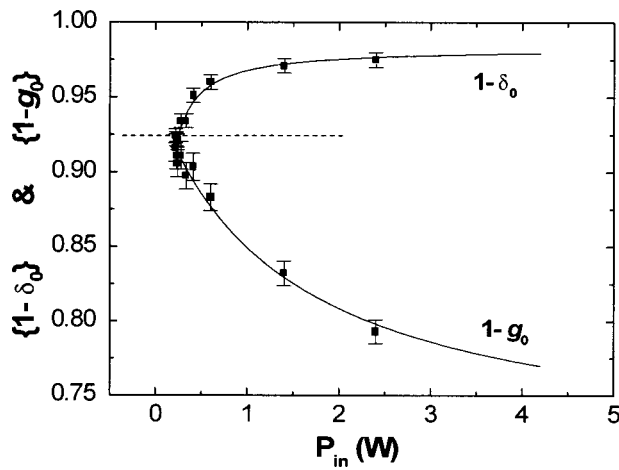


FIG. 4. Measured values of unsaturated gain and resonator losses from Table I. The fitted curve is obtained by using an empirical function of the form $(1 - \delta_0) = A * P_{in} / (B + P_{in})$.

be made, based on a crude fitting of the data with an empirical function of the form $(1 - \delta_0) = A * P_{in} / (B + P_{in})$ and a similar function for the unsaturated gain. The fitting results are given in the graphs and lead to estimated values at high pump power ($P_{in} = 10$ W) of $\delta_0 = 0.022$ and $g_0 = 0.34$.

The predicted values of $g_0 = 0.34$ and $\delta_0 = 0.022$ for the high pump power will be used with a certain degree of caution. The reason of interest for the high gain case is the possibility of using 10 W input power to the dye laser, even though most practical systems become unstable at these high pump powers.

D. Low gain conditions

When substituting the gain and loss values for $P_{in} = 230$ mW, $g_0 = 0.089$, and $\delta_0 = 0.078$ into Eqs. (6) and (15), respectively, one obtains curves for $W_{abs}^{ext'}$ and $W_{abs}^{int'}$ as a function of optical density for various values of N , the number of passes in the extra-cavity scheme, as depicted in Fig. 5. It is assumed that the loss due to the sample cell windows in one roundtrip, $\delta_{cell} = 0.004$ (0.001 per pass through a window) and that the transmission and reflectivity of the relevant optics in the EC scheme = 0.999. $(\delta_e)_{opt}$ is estimated from Eq. (14) to be 0.0053. It is further assumed that the parasitic absorbance due to the solvent is negligible.

It can be seen that for a single pass EC scheme, the IC scheme is more efficient for the values of optical density presented. Even for $N = 50$ the IC scheme is more efficient for optical densities up to ~ 0.006 . At the optical density of 0.007 the IC scheme is at the lasing threshold. The IC absorbed intensity $W_{abs}^{int'}$ has a maximum value of 1.45×10^{-4} at an optical density of 0.0035, whereas $W_{abs}^{ext'}$ has a maximum value of 4.5×10^{-4} which is reached asymptotically at higher optical densities, depending on the number of passes. Hence $W_{abs}^{int'}$ has reached only $\sim 30\%$ of the maximum value obtainable for $W_{abs}^{ext'}$. Although using low pump power would not result in an overall high cooling rate, it follows from Fig. 5 that intracavity laser cooling results in higher cooling efficiency in this case. This is evident once more

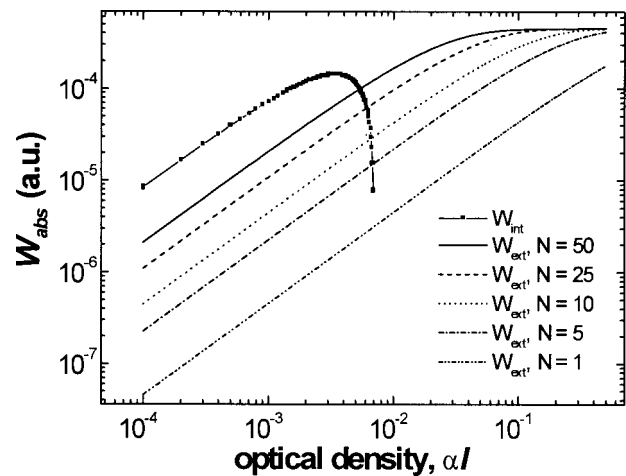


FIG. 5. Absorbed intensity, W_{abs} , in the IC and EC schemes as a function of the number of passes N in the EC scheme. The curves are established using Eqs. (6) and (15) for low pump power (230 mW), based on the estimated values for laser gain and losses of $g_0 = 0.089$ and $\delta_0 = 0.078$ and using the value of $\delta_{cell} = 0.004$. For $\alpha l > \sim 0.007$ the IC scheme is below lasing threshold.

from Fig. 6, which shows the number of passes in the EC scheme that makes the values of $W_{abs}^{ext'}$ and $W_{abs}^{int'}$ equivalent, as a function of optical density, αl .

E. High gain conditions

In the case of the high gain situation (10 W pump power), where predicted values of $g_0 = 0.34$ and $\delta_0 = 0.022$ are used, the data in Fig. 7 are obtained. At an optical density of 0.18 the IC scheme is equivalent to the EC scheme of 1 single pass. Figure 8 shows the number of equivalent passes in the EC scheme for the high gain case as a function of αl . The IC absorbed intensity $W_{abs}^{int'}$ has a maximum value of 0.184 at an optical density of 0.08, whereas $W_{abs}^{ext'}$ has a maximum value of 0.76 at higher optical densities, again depending on the number of passes. This means that $W_{abs}^{int'}$ has reached only $\sim 20\%$ of the maximum value obtainable for $W_{abs}^{ext'}$. From these data it follows that when using high

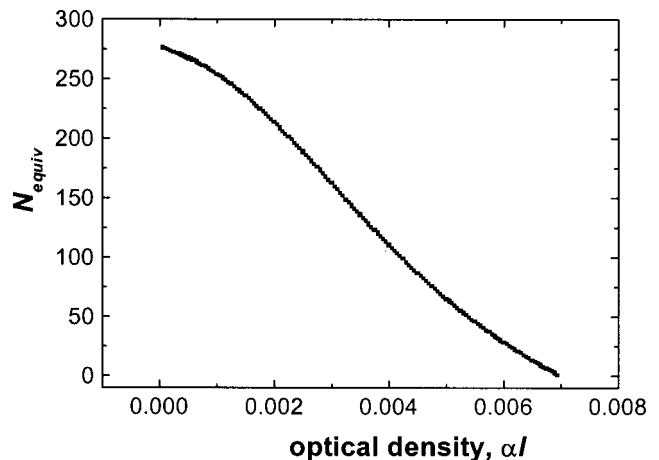


FIG. 6. Equivalent number of passes as a function of optical density in the low gain IC and EC schemes, based on the values in Fig. 5.

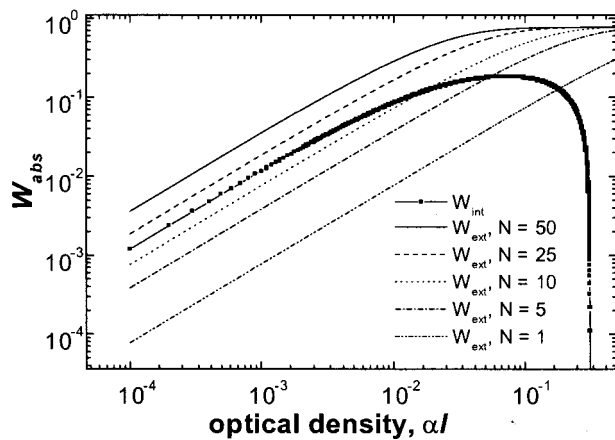


FIG. 7. Absorbed intensity, W_{abs} , in the IC and EC schemes as a function of the number of passes N in the EC scheme. The curves are established using Eqs. (6) and (15) for high pump power (10 W), based on the estimated values for laser gain and losses of $g_0=0.34$ and $\delta_0=0.022$ and using the value of $\delta_{cell}=0.004$. For $\alpha/l > \sim 0.3$ the IC scheme is below lasing threshold.

pump power and optical densities, optical cooling is achievable with higher efficiency in the multipassing extra-cavity scheme than in the intracavity scheme.

It follows from the data presented in Figs. 7 and 8 that for the laser system parameters (gain and losses) described at high pump power, only for low optical densities (<0.01) does the IC scheme compete with the EC scheme due to the difficulty of multipassing >50 times through a condensed material. Laser cooling in the condensed phase can only work at wavelengths where the extinction coefficient happens to be small, however, since the extinction coefficient is ~ 0.11 at 10^{-4} M at the wavelength of interest of 620 nm,² this sample would then, from the predictions represented in Fig. 8, be as easy to cooldown in two passes in the EC configuration as in an IC configuration. Although when using a longer path length cell increased reabsorption effects can be expected, which are not included in the analysis presented here, these effects are present in both the EC and the IC scheme and do therefore not alter the main discussion.

Other factors will change the situation presented in Figs. 5–8. For instance, when introducing a birefringent element for wavelength tuning, the inclusion of the extra losses will affect the IC scheme more than the EC scheme. Also, due to the polarization of radiation inside the laser resonator, the effective absorption cross section will be slightly lower in the IC scheme. This is not necessarily a problem in the EC scheme as the laser output can be depolarized before entering the multipass cell.

The comparison presented in this article between an extra- and an intra-cavity laser cooling configuration is based only on the attenuation of light based on Beer's law. Other factors, such as the reabsorption of fluorescence, are considered to affect the cooling efficiency in a similar fashion, as the geometry of the samples is considered to be equal for both the EC and IC schemes. Further, the existence of a thermal lens in the sample has not been taken into account in this comparative analysis and can be expected to alter the

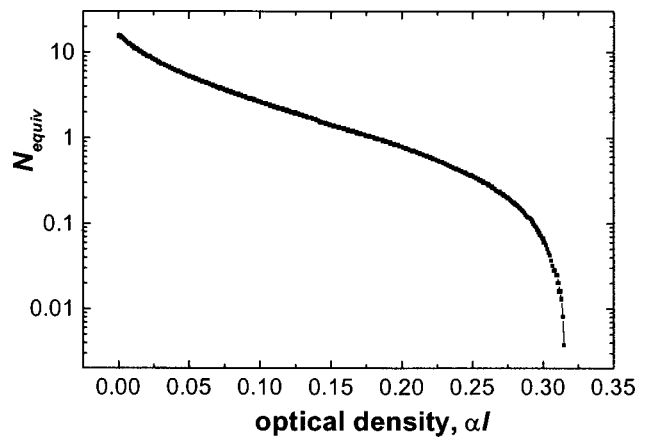


FIG. 8. Equivalent number of passes as a function of optical density in the high gain IC and EC schemes, based on the values in Fig. 7.

calculated cooling efficiencies. However, in order to estimate the relative merit of an IC versus EC cooling configuration it has been assumed that the thermal lens will be of comparable magnitude in both cases. This is not strictly the case, since the lensing is directly proportional to the intensity profile of the beam traveling through the sample and will be different in each case.

V. CONCLUSION

A comparison of the maximum absorbed intensity for a sample inside and outside a laser cavity is reported. From the analysis, at high dye laser input power it follows that the IC scheme is preferred when employing low optical density (<0.01) samples, whereas the EC scheme is preferred for higher optical densities (>0.1).

The present analysis is based on estimated values for the gain and loss factors of a dye laser and is therefore limited to this particular system, but the method is considered to be applicable to other laser systems. It has also been pointed out that implementing reabsorption and thermal lens effects will provide a more realistic picture of the cooling efficiency of an intra- versus an extra-cavity cooling device and as such the inclusion of these effects can be regarded as improvements to the present analysis.

The analysis presented in this article is based on a comparison of absorbed intensities of radiation as a function of optical densities of the cooling medium for a given input power to the dye laser and as such does not distinguish between the separate contributions to the optical density, concentration, and path length. Increased reabsorption of radiation at higher concentrations means that two different cooling samples with equal optical densities, but a different combination of concentration and path length, do not necessarily result in the same cooling efficiency in practice, be this by intra- or extra-cavity laser cooling. However, since it has been assumed that the geometry of the cell is the same in both cases for a given optical density, geometry related effects such as reabsorption and thermal lensing are only important when optimizing the geometry of one of the configurations individually. Based on the present analysis being concerned only with the comparative efficiencies between

the two types of cooling configurations for a given geometry, these effects can be treated in a separate analysis.

ACKNOWLEDGMENTS

The authors would like to thank the Physics College of the Engineering and Physical Sciences Research Council (EPSRC) in the U.K. for provision of funds for this work through Grant No. GR/L84179. This effort was partially sponsored by the United States Air Force, Air Force Materiel Command, Air Force Research Laboratory, Phillips Research Site, 3550 Aberdeen Avenue, SE, Kirtland AFB, NM 87117-5776.

¹R. I. Epstein, M. I. Buchwald, B. C. Edwards, T. R. Gosnell, and C. E. Mungan, *Nature (London)* **377**, 500 (1995).

- ²J. L. Clark and G. Rumbles, *Phys. Rev. Lett.* **76**, 2037 (1996); J. L. Clark, P. F. Miller, and G. Rumbles, *J. Phys. Chem. A* **102**, 4428 (1998).
- ³E. Finkeifen, M. Potemski, P. Wyder, L. Viña, and G. Weimann, *Appl. Phys. Lett.* **75**, 1258 (1999).
- ⁴T. R. Gosnell, *Opt. Lett.* **24**, 1041 (1999).
- ⁵B. C. Edwards, J. E. Anderson, R. I. Epstein, G. L. Mills, and A. J. Mord, *J. Appl. Phys.* **86**, 6489 (1999).
- ⁶A. Rayner, M. E. J. Friese, A. G. Truscott, N. R. Heckenberg, and H. Rubinsztein-Dunlop, *J. Mod. Opt.* **48**, 103 (2001).
- ⁷B. C. Edwards, M. I. Buchwald, and R. I. Epstein, *Rev. Sci. Instrum.* **69**, 2050 (1998).
- ⁸G. Lamouch, P. Lavallard, R. Suris, and R. Grousson, *J. Appl. Phys.* **84**, 509 (1998).
- ⁹R. Frey, F. Micheron, and J. P. Pocholle, *J. Appl. Phys.* **87**, 4489 (2000).
- ¹⁰B. Heeg and G. Rumbles, *J. Appl. Phys.* (submitted).
- ¹¹A. E. Siegman, *Lasers* (University Science Books, Sausalito, 1986).
- ¹²E. Puig Maldonado, G. E. Calvo Noguiera, and N. Dias Vieira, *IEEE J. Quantum Electron.* **29**, 1218 (1993).